A Novel Intersubunit Communication Mechanism in a Truncated Hemoglobin from *Mycobacterium tuberculosis*

Syun-Ru Yeh*

Department of Physiology and Biophysics, Albert Einstein College of Medicine, Bronx, New York 10461

Received: October 9, 2003; In Final Form: November 13, 2003

HbN is a homodimeric hemoglobin from *Mycobacterium tuberculosis* that belongs to the newly discovered truncated hemoglobin family. The intersubunit communication mechanism in HbN was investigated by ligand replacement experiments, in which the heme-bound CO in the fully CO-saturated dimer was gradually replaced with oxygen, and vice versa. A mixed-ligand species, in which one subunit binds a CO molecule and the other subunit binds an oxygen molecule, was formed under relatively low CO concentrations. The CO-bound subunit in the mixed-ligand species was found in the open conformation, in contrast to an equilibrium mixture of open and closed conformations in the fully CO-saturated derivative. On the other hand, the O_2-bound subunit stays in the closed conformation regardless of the saturation level of CO. These observations suggest that the formation of the H-bonds between the B10 tyrosine and the heme-bound dioxygen in one subunit of the dimer forces its neighboring CO-bound subunit to adopt an open conformation. The new data reported here not only reveal a novel intersubunit communication mechanism but also provide the first experimental evidence for an intermediate ligation state that is critical for a ligand-linked allosteric structural transition.

Introduction

Hemoglobins are widely distributed among prokaryotes, unicellular eukaryotes, plants and animals.[1−9] They are considered as the paradigm for understanding the molecular mechanisms underlying allosteric transitions in proteins.[10−18] In the animal kingdom, it is well-known that hemoglobin serves as an oxygen carrier that delivers oxygen to local tissues through the vascular system. The hemoglobin found in the perienteric fluid of the worm *Ascaris suum*, on the other hand, is a NO-dependent deoxygenase.[19,20] It uses endogenously produced NO to detoxify oxygen, which is poisonous to the fully anaerobic mitochondrial oxidation pathway in the *Ascaris* worm. For leghemoglobin found in root nodules of legumes, a similar role has been proposed for keeping the symbiotic nitrogen-fixing bacterium anaerobic and protecting the nitrogen-fixing enzyme system from oxidation.[4,21] In addition to the deoxygenase activity, it is well accepted that leghemoglobin also facilitates oxygen diffusion to terminal oxidases of the symbiotic bacteria.[4,21,22] The flavohemoglobins from *E. coli* or yeast detoxify NO through an oxygen-dependent NO dioxygenation reaction or an oxygen-independent NO reduction reaction, thereby protecting the cells against nitrosative stress under aerobic or anaerobic conditions, respectively.[23−27] Recently, a new hemoglobin-like dehaloperoxidase was found in a marine worm, *Amphitrite ornate*, which is capable of dehalogenasing bromophenols produced by other worms. It adds a new dimension to the catalytic functions of hemoglobins.[28,29]

The diversity of the functional properties of hemoglobins relies on small variations in the amino acid residues lining the heme pocket because they all share the same prosthetic group.[1,2,30−32] On the other hand, the ligand binding linked allosteric structural transition of hemoglobins relies on the assemblage of the subunits into oligomers.[1,3,10−16] The quaternary assemblage of hemoglobin subunits is remarkably diverse, ranging from the monomeric hemoglobins of bacteria to the 144 subunits of gigantic annelid extracellular hemoglobin.[1,3] In tetrameric human hemoglobin, ligand binding to the heme iron induces structural changes in the proximal iron−histidine bond in one subunit, which is transmitted to the other subunits through an allosteric structural transition involving a cascade of events.[14,33,34] In the homodimeric hemoglobin from the arcid clam, *Scapharca inaequivalvis*, the intersubunit contact region is formed by the two heme-carrying E and F helices, and the intersubunit communication is mediated by localized structural changes near the heme pockets without substantial quaternary structural rearrangements.[15,35,36] In both mechanisms, the allosteric transition is triggered by movement of the heme iron into the porphyrin plane upon ligand binding. In contrast, in the homodimeric hemoglobin from sea lamprey, there is no significant structural rearrangement on the proximal side in response to ligand binding.[37] It was proposed on the basis of crystallographic data that the allosteric mechanism in the lamprey hemoglobin is solely controlled by distal interactions involving the movement of a distal histidine residue.

The wide array of newly discovered hemoglobins adds a new twist to the scope of allosteric transition mechanisms.[2,7,38] Based on sequence alignments, two groups of hemoglobins have been identified in unicellular organisms. The first group consists of flavohemoglobins from bacteria and fungi, which have a hemoglobin domain with a classical three-over-three α-helical sandwich motif and a flavin-containing reductase domain that is either covalently or noncovalently associated with the hemoglobin domain. The second group, termed truncated hemoglobin, is characterized by a novel two-over-two α-helical sandwich motif, the absence of the A and D helices, and the presence of an extended loop substituting for most of the F helix.[39−41] Among these hemoglobins, a homodimeric truncated hemoglobin, HbN, from *Mycobacterium tuberculosis*, is especially interesting.[42,43] Spectroscopic and biochemical studies suggest that the primary role of HbN is to protect the bacilli

* E-mail address: syeh@aecom.yu.edu.

10.1021/jp037054q CCC: $27.50
Published on Web 12/30/2003

against NO produced by the host macrophage during latency.[42−45] The proximal ligand to the heme in HbN is histidine, the universally conserved proximal ligand among the super family of hemoglobins. The distal residues at the E7 and B10 positions, which stabilize heme-bound ligands in other hemoglobins, are leucine and tyrosine, respectively. Resonance Raman spectroscopy along with mutagenesis studies revealed that the heme-bound oxygen is stabilized through H-bonding interactions with the distal B10 tyrosine.[42] This proposal was later confirmed by crystallographic studies.[39] On the other hand, the CO-bound protein was found to have two conformations with characteristic Raman bands (ν_{Fe-CO}) at 500 and 535 cm^{-1}.[42] They were assigned to an open and a closed conformation, respectively. In the closed conformation, the heme-bound CO forms a H-bond with the B10 tyrosine. This H-bond is absent in the alternative open conformation. In this work, the two ν_{Fe-CO} bands were used as structural marker lines to examine the ligand-linked intersubunit communication mechanism in HbN.

Experimental Procedures

Recombinant *Mycobacterium tuberculosis* HbN was cloned, expressed, and purified to near homogeneity as described elsewhere.[43] The protein was buffered with 50 mM Tris buffer at pH 7.5. The Raman measurements with Soret excitation were made with previously described instrumentation.[42] Briefly, the output at 406.7 nm from a krypton ion laser (Spectra Physics) was focused to a ~30 μm spot (laser power ≈ 2 mW) on a rotating cell to prevent photodamage to the sample. The scattered light was collected at right angles to the incident beam and focused on the entrance slit of a 1.25 m polychromator (Spex) where it was dispersed and then detected by a charge-coupled device (Princeton Instruments). The protein concentration was 50 μM. The acquisition time was about 30 min for each spectrum. The Raman spectra were calibrated with indene (Sigma). Optical absorption spectra were acquired before and after spectral acquisition to ensure that there is no photodamage occurring to the sample during the spectral acquisition.

Results

The Fe−O_2 stretching frequency of the oxy derivative of HbN was identified at 560 cm^{-1} with resonance Raman spectroscopy, a lower frequency than that of mammalian globins (~570 cm^{-1}), due to the presence of two H-bonds between the B10 tyrosine and both oxygen atoms of the heme-bound dioxygen.[42] The presence of the H-bonding interaction was confirmed by the crystallographic data[39] and by the observations that mutation of the B10 tyrosine to a phenylalanine causes the Fe−O_2 stretching mode to shift to 570 cm^{-1} and the oxygen dissociation rate to increase by 150-fold.[42] Whereas the oxy derivative of HbN displayed only one Fe−O_2 stretching mode, two Fe−CO stretching modes, at 500 and 535 cm^{-1}, were identified in the fully saturated CO derivative.[42] They were assigned to an open and a closed conformation, respectively. The intensity ratio of these two modes is independent of pH, protein concentration (from 5 to 50 μM), and incident laser power. Mutagenesis studies show that the vibrational mode at 535 cm^{-1} disappears upon the B10 tyrosine to phenylalanine mutation, confirming that in the closed conformation the B10 tyrosine forms a H-bond with the heme-bound CO.[42] On the other hand, this H-bonding interaction is absent in the open conformation. The presence of the two conformations in the CO derivative suggests that the H-bond between the heme-bound CO and the B10 tyrosine is not strong enough to lock the conformation in the closed conformation. It also demonstrates the plasticity of the structure of the CO derivative with respect to the oxy derivative.

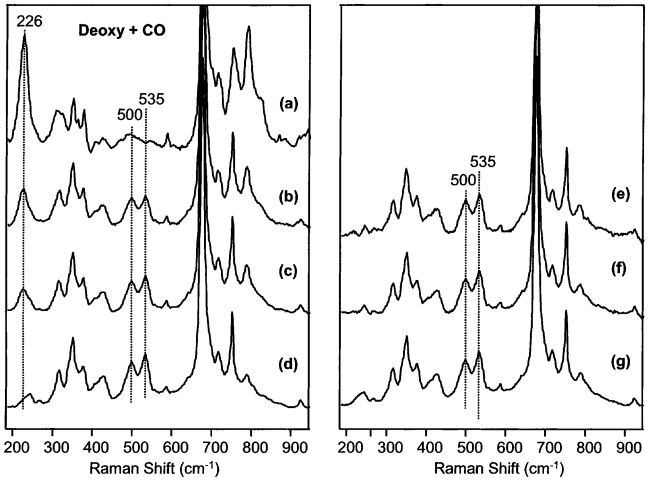

Figure 1. The low-frequency Raman spectra (a−d) of the ferrous forms of HbN at pH 7.5 in the presence of increasing amounts of CO and the net Raman spectra (e−g) of the ferrous carbon monoxide derivative of HbN obtained by subtracting out the spectral contribution of the ferrous deoxy species (trace a) from the traces b, c, and d, respectively.

CO Titration of the Deoxy-HbN. To evaluate the effect of CO binding to one subunit of the dimer on the conformation of the neighboring subunit, the deoxy derivative was titrated with CO. Figure 1a−d shows the resonance Raman spectra of the dimer in the presence of an increasing concentration of CO. The decrease in the 226 cm^{-1} band, the iron−histidine stretching mode of the deoxy protein, and the concomitant increase in the intensities of the 500 and 535 cm^{-1} bands associated with the CO derivative reflect the coordination of CO to the deoxy protein. To extract the pure spectrum of the CO derivative built up during the titration, the spectral contribution from the deoxy species (Figure 1a) was subtracted from each spectrum shown in Figure 1b−d. The resulting spectra are shown in Figure 1e−g, respectively. The data show that the intensity ratio of the 500/535 cm^{-1} bands is invariant with respect to the degree of saturation with CO. It indicates that the open and closed conformations are in the same thermodynamic equilibrium regardless of the saturation level of CO.

Ligand Replacement Experiments. To investigate the intersubunit communication in dimeric HbN, ligand replacement experiments were performed, in which the heme-bound CO in the CO derivative was replaced with O_2 stepwise. It was found that the increase in the spectral contribution from the oxy derivative is associated with a decrease in the intensities of the 500 and 535 cm^{-1} bands (for raw data see Figure 1 in the Supporting Information). To obtain the pure spectrum of the CO derivative in the mixture, the spectral contribution from the oxy derivative was subtracted from each raw spectrum. The resulting net spectra are shown in Figure 2a−d with increasing O_2 concentration. The data show that the relative intensity of the 500 cm^{-1} band increases as the concentration of O_2 increases. In addition, in the presence of relatively high concentrations of oxygen, only the open conformation was observed (Figure 2d). To interpret these resonance Raman data, the sequential changes to the heme ligation states during the ligand replacement experiments are illustrated in the right panel of Figure 2. As shown in the cartoon, the dominating CO species under high oxygen concentrations is associated with the *mixed-ligand dimer*, in which one heme binds an O_2 molecule and the other binds a CO molecule. On the basis of this analysis, the

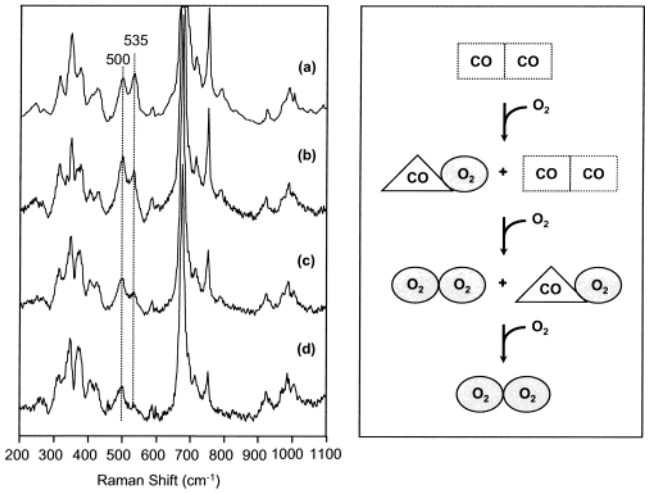

Figure 2. In the left panel, the net Raman spectra (a−d) of the ferrous carbon monoxide derivative of HbN at pH 7.5 obtained by subtracting out the spectral contribution of the oxy derivative in the ligand replacement experiment in which the CO in the carbon monoxide derivative is replaced by O_2 stepwise as increasing amounts of O_2 are added to the solution from trace a to trace d. The two Fe−CO stretching modes at 500 and 535 cm^{-1} are assigned as open and closed conformations, respectively, and in the right panel, a pictorial illustration of the ligand replacement experiment between O_2 and CO. The fully CO-saturated derivative is in a thermal equilibrium state between an open and a closed conformation as indicated by the dotted rectangular box. A *mixed-ligand dimer* in which one heme binds an oxygen molecule and the other binds a CO molecule was identified in the presence of low and medium concentrations of O_2. The structure of the CO-coordinated subunit in the mixed-ligand dimer is locked in an open conformation as indicated by the transformation from the dotted rectangular box to a triangular box.

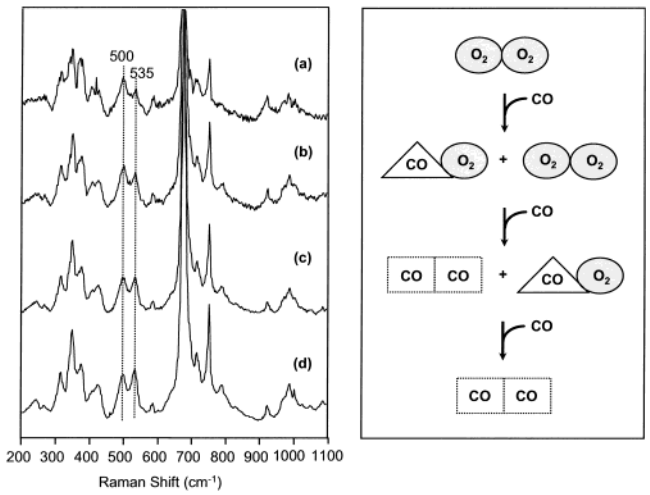

Figure 3. In the left panel, the net Raman spectra (a−d) of the ferrous carbon monoxide derivative of HbN at pH 7.5 obtained by subtracting out the spectral contribution of the oxy derivative in the ligand replacement experiment in which the O_2 in the oxy derivative is replaced by CO stepwise as increasing amounts of CO are added to the solution from trace a to trace d and, in the right panel, a pictorial illustration of the ligand replacement experiment between O_2 and CO. The fully CO-saturated derivative is in a thermal equilibrium state between an open and a closed conformation as indicated by the dotted rectangular box. A *mixed-ligand dimer* in which one heme binds an oxygen molecule and the other binds a CO molecule was identified in the presence of low and medium concentrations of O_2. The structure of the CO-coordinated subunit in the mixed-ligand dimer is locked in an open conformation as indicated by the transformation from the dotted rectangular box to a triangular box.

resonances Raman data indicate that the CO derivative in the mixed-ligand dimer prefers the open structure.

To test the model presented in Figure 2, the heme-bound O_2 in the fully saturated oxy derivative was resubstituted with CO. Figure 3a−d shows the net spectra of the CO derivative extracted from the raw data (for raw data see Figure 2 in the Supporting Information) by subtracting out the spectral contribution from the oxy derivative. The corresponding sequential changes to the heme ligation states during the ligand replacement experiments are illustrated in the right panel of Figure 3. Again, the 500 cm^{-1} band is dominant under relatively high oxygen concentrations, when the mixed-ligand dimer is highly populated. It confirms that the CO derivative in the mixed-ligand dimer prefers the open structure. In both ligand replacement experiments shown in Figures 2 and 3, the Fe−O_2 stretching frequency stays invariant at 560 cm^{-1} regardless of the saturation level of CO, demonstrating that O_2 forms a hydrogen bond with the B10 tyrosine independent of the ligation state of the neighboring subunit in the dimer.

Discussion

The stabilization of heme-bound O_2 by a tyrosine residue at the B10 position through H-bonding interactions has also been observed in several hemoglobins other than HbN as listed in Table 1. All of the wild-type proteins shown in Table 1, except sperm whale myoglobin, exhibit a low Fe−O_2 stretching frequency. This has been attributed to the presence of H-bond(s) between the B10 tyrosine and the heme-bound O_2. Like HbN, the mutation of the B10 tyrosine to leucine in the *Chlamydomonas* hemoglobin causes an upshift of the Fe−O_2 stretching frequency, reflecting the loss of the H-bond(s). Due to the specific stereo-orientation of the side chain group of the B10 tyrosine with respect to the heme-bound ligands and the preferential linear structure of the Fe−C−O moiety with respect to the bent structure of the Fe−O−O moiety, the presence of a stabilization between the heme-bound O_2 and the B10 tyrosine does not necessarily indicate the existence of a similar stabilization of the heme-bound CO by the B10 tyrosine. For instance, the CO may be stabilized by the B10 tyrosine in HbN, *E. coli* Hmp, and barley Hb, but not in HbO, *Chlamydomonas* Hb, *Paramecium* Hb, and *Synechocystis* Hb.

TABLE 1: The Frequencies of the Iron−CO (Fe−CO), C−O, and Iron−O_2 (Fe−O_2) Stretching Modes of Various Hemoglobins with a Tyrosine Residue at the B10 Position[a]

proteins	type	υ_{Fe-CO}	υ_{C-O}	υ_{Fe-O2}	refs
M. tuberculosis HbN	wild type	500, 535	1960, 1916	560	42
	B10 Y→F	502		570	42
Chlamydomonas Hb	wild type	491		556	51, 52
	B10 Y→L			561	52
E. coli Hmp	wild type	494, 535	1960, 1907		46
barley Hb	wild type	493, 534	1960, 1924		53
Paramecium Hb	wild type	491	1974	563	54
Synechocystis Hb	wild type	492	1955	554	52, 55
sperm whale Mb	wild type	507	1947	569	56

[a] Those of sperm whale myoglobin are listed as references.

The presence of two conformations in the CO derivative demonstrates that the distal pocket of HbN is flexible and it can fluctuate between an open and a closed conformation. Similar dual structures have been observed in the CO derivatives of the hemoglobin from *Ascaris suum* and the flavohemoglobin from *E. coli*.[46,47] One common feature in these hemoglobins, including HbN, is that they are all implicated in performing NO/O_2 chemistry physiologically. It is plausible that the flexible distal pocket in these hemoglobins is tailored to perform oxygen chemistry, instead of a conventional role in oxygen delivery.

Stepwise titration of the deoxy derivative of HbN with CO showed that the ratio between the open and the closed conformation is invariant regardless of the saturation level of CO. It is conceivable that CO binding is highly cooperative and the dimeric protein is always fully saturated with CO with one subunit in the open conformation and the other in the closed conformation regardless of the CO concentration. The preference of the open structure for the CO derivative in the mixed-ligand dimer, on the other hand, may be interpreted by the preferential displacement of the CO in the closed conformation with O_2 during the ligand exchange reactions. However, this scenario is ruled out because the presence of the strong H-bonding interaction between the B10 tyrosine and the CO in the closed conformation makes it unlikely that O_2 could preferentially replace the CO in the closed conformation. Instead, the data suggest that O_2 replaces the CO in the subunit with open conformation and the formation of the new H-bonds between the heme-bound dioxygen and the B10 tyrosine in this subunit forces its neighboring CO-bound subunit to adopt an open conformation. A possible molecular mechanism underlying the intersubunit communication is discussed below.

Molecular Mechanism for the Intersubunit Communication. In the previous resonance Raman studies, it was shown that the proximal Fe−His bond in the deoxy derivative of HbN is significantly stronger than that of mammalian globins on the basis of a higher Fe−His stretching frequency (226 vs 216 cm^{-1}).[42] The high Fe−His stretching frequency of HbN is consistent with an unstrained proximal histidine. The unstrained proximal histidine in HbN suggests that the intersubunit communication observed in the mixed-ligand species is not mediated by the conformational changes on the proximal side of the heme as that observed in human hemoglobin. This proposal is further confirmed by nanosecond flash photolysis experiments showing that the proximal iron−histidine stretching frequency of the nanosecond photoproduct of the CO derivative of HbN is identical to that of the equilibrium ligand-free form (to be published).

To understand the intersubunit communication mechanism in the context of the protein structure, the crystal structure of the oxy derivative of HbN (PDB code: 1IDR), the only crystal structure available for this protein,[39] was examined. According to the crystal structure, HbN forms a head-to-tail dimer, as shown in Figure 4, which is stabilized by the H-bonding interactions between the pre-F helix loop in the subunit B and the Arg-35 at the B12 position in the subunit A. As further illustrated in Figure 5, the heme-bound dioxygen is stabilized by H-bonding interactions with the Tyr-33 at the B10 position, which in turn forms a H-bond with the Gln-58 at the E11 position. The Arg-53 at the E6 position, located approximately one helical turn away from the E11 (Gln 58) residue, forms a H-bond with a heme propionate group. This heme propionate group also forms a H-bond with the backbone amine group of the Ala-75 residue, located in the pre-F helix loop. The carbonyl group of the Ala-75 in turn forms a H-bond with the tyrosine-72 residue. More importantly, this pre-F helix loop containing residues 72−75 in the subunit B forms two H-bonds with the Arg-35 at position B12 in the subunit A, which is only a half helical turn away from the B10 Tyr-33 residue. It is plausible that the intersubunit communication in the mixed-ligand species observed during the ligand replacement experiments is mediated by these sophisticated H-bonding networks linking the distal ligand binding sites together in the novel head-to-tail dimer.

Although the Fe−O_2 stretching frequency found in the oxy derivative indicates only one conformation,[42] it is evident from

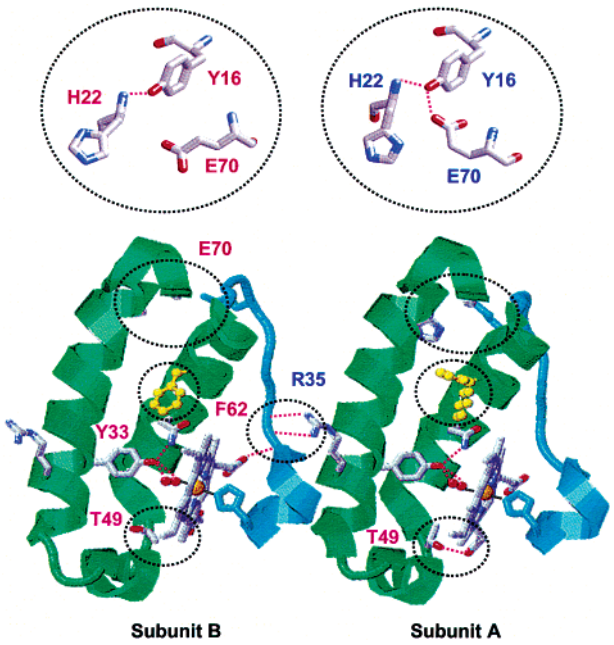

Figure 4. The crystal structure of HbN (PDB code: 1IDR) illustrating the intersubunit interactions. For clarity, only residues 16−81 are shown. The B, D, and E helices are labeled as green, and the pre-F helical loop and the F helix are labeled as cyan. HbN is a head-to-tail dimer with the interface stabilized through two H-bonds between the pre-F helix loop in the B subunit and the Arg-35 in the A subunit. In addition, the two subunits have slightly different structures as highlighted by the dotted circles and illustrated in Figure 5. Phe-62 is labeled in a ball-and-stick model to demonstrate its increased conformational freedom in the subunit A. The inserts illustrate the chemical environments of the E70 structural region in the A and B subunits. The H-bonds are represented by dotted lines.

the crystal structure that the H-bonding network between the B10 Tyr-33, the E11 Gln-58, and the heme-bound dioxygen is slightly different in the subunit A as compared to that in the subunit B, as reflected by the longer Fe−O_2 bond, the longer H-bond between the B10 Tyr-33 and the heme-bound O_2, and that between the B10 Tyr-33 and the E11 Gln-58 in the subunit A. It is conceivable that the H-bonding network in one subunit induces an allosteric structural transition that causes the weakening of the H-bonding network in the counterregion in the other subunit. The structural transition is manifested in four structural features in the subunit A that are absent in the subunit B: (1) the H-bonds between the B7 Glu-30 and the E8 Lys-55 (see Figure 5) due to the change in the side chain conformation of the Lys-55 residue; (2) the H-bond between the Tyr-16 and the Glu-70 (see the inserts in Figure 4), which are located at the end of the B and E helices, respectively, as a result of a large scale movement of the side chain group of the Glu-70 residue; (3) the H-bond between the side chain group of Thr-49 in the linker region between the B and E helices and a heme propionate group (Figures 4 and 5) as a result of the movement of both the Thr-49 side chain group and the propionate group; (4) an increase conformational freedom in the side chain group of the Phe-62 at the E15 position (Figure 4), as indicated by the two alternative conformations observed in the subunit A that are not present in the subunit B.

Taken together, these data suggest that the H-bonding network, mediated by the B and E helices and the pre-F helix loop, provides a direct route for the communication between the two heme groups in HbN. It is plausible that in the mixed-ligand species the O_2 and CO molecules bind to the B and A subunits, respectively. The strong hydrogen bonds between the

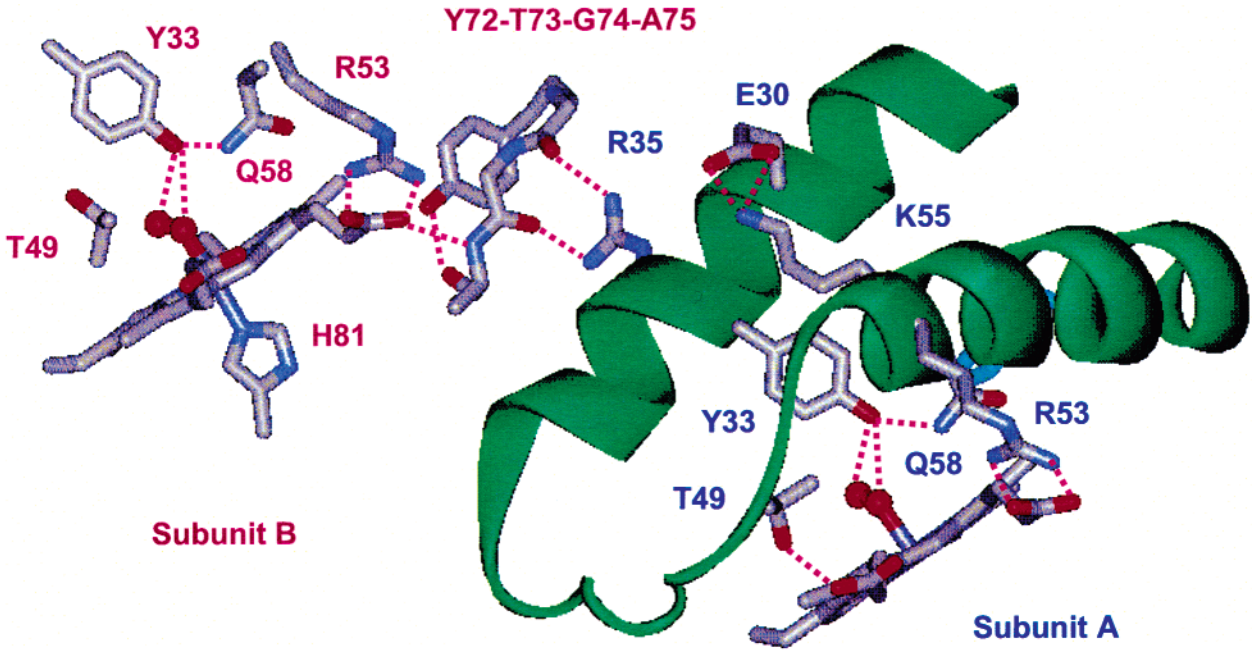

Figure 5. The structure of HbN (PDB code: 1IDR) illustrating a possible route for the intersubunit heme−heme communication as discussed in the text. The H-bonds are represented by dotted lines.

B10 Tyr-33 and the heme-bound O_2 bring both the B and E helices closer to the heme iron because the B10 Tyr-33 is stitched to the E11 Gln-58 through a strong H-bond. The movement of the B and E helices toward the heme iron in the B subunit is transmitted to the subunit interface through the E6 Arg-53, the heme propionate group, and the pre-F helix loop region (Figure 5). It is further passed onto the subunit interface, which is secured by H-bonds between the pre-F helix loop region and the B12 Arg-35 residue, and finally to the B−E helices in the neighboring CO-bound subunit A. As a result, the B and E helices pack more tightly as reflected by the new H-bonds in the Lys-55 structural region (see subunit A in Figure 5) and the Glu-70 region (see subunit A in Figure 4). In addition, it brings the linker region between the B and E helices closer to the heme propionate group, as reflected by the new H-bond in the Thr-49 structural regions. These structural changes create an enlarged space between the B−E helices and the heme plane as reflected by the increased conformational freedom of the Phe-62 residue and, more importantly, an open conformation for the Fe−CO moiety. Because of the plasticity of the dimeric structure, a similar intersubunit communication mechanism can be applied to the mixed-ligand dimer with bound O_2 and CO in the subunits A and B, respectively, in which the structural transition is transmitted from the subunit A to subunit B. Based on these long-range interactions, the following two possible ligand binding linked communication mechanisms are proposed.

A Three-State Model. In the three-state model, the deoxy derivative fluctuates between an open and a closed conformation (Figure 6a). When one subunit of the dimer adopts the open conformation, a ligand can coordinate to the heme. If it binds an O_2 molecule, the strong hydrogen bonding between O_2 and the B10 tyrosine forces its distal heme pocket to close. The enclosure of the heme pocket around the bound O_2 introduces topological changes in this subunit, which subsequently force the neighboring deoxy subunit to adopt an open conformation (Figure 6b) through an allosteric structural transition. If the second member of the dimer binds an O_2 molecule, the new strong hydrogen bonding between O_2 and the B10 tyrosine causes its distal heme pocket to close (Figure 6c). On the other hand, if the second member of the dimer binds a CO molecule instead of O_2, it forms the mixed-ligand dimer (Figure 6d).

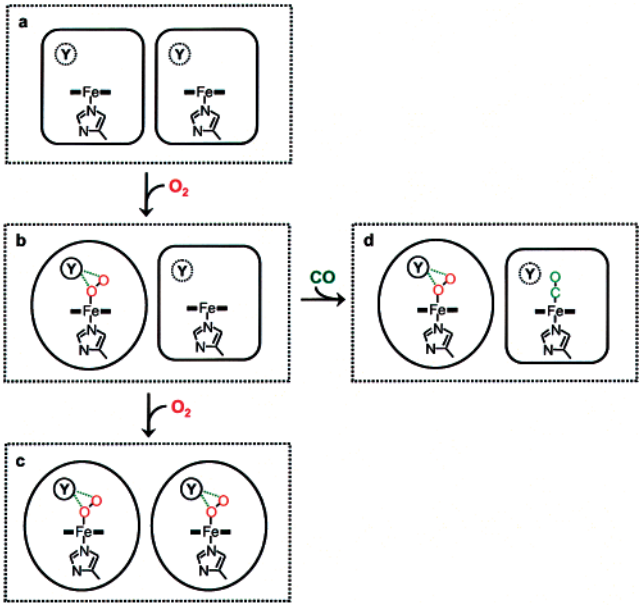

Figure 6. In the three-state model, the ferrous deoxy species fluctuates between an open and a closed conformation, although only the open structure is shown here (panel a). When one of the two subunits binds an oxygen molecule, the distal B10 tyrosine (labeled as Y) forms two H-bonds with the heme-bound dioxygen causing the distal pocket to close down. This allosteric structural transition is transmitted to the neighboring subunit and forces it to adopt an open conformation (panel b). If the second subunit binds another oxygen molecule, an additional structural transition occurs, and as a result, both subunits adopt a closed conformation (panel c). On the other hand, if the second subunit binds a CO molecule, it forms a mixed-ligand dimer (panel d). In the mixed-ligand dimer, the CO-bound subunit preserves the open conformation because the H-bond between the CO and the B10 tyrosine is not strong enough to lock the structure in the closed conformation. The distinct quaternary structure of each subunit in the various ligation states of the HbN dimer is schematically illustrated by a square-shaped or a circular-shaped subunit, representing the open and closed conformation, respectively.

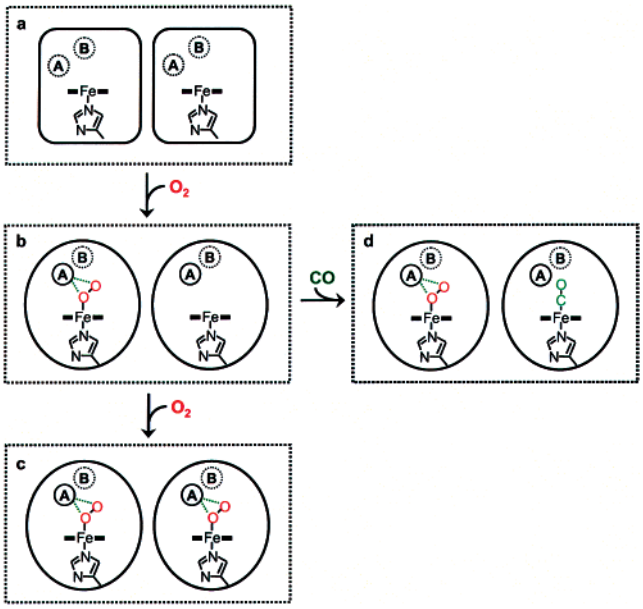

Figure 7. In the two-state model, the B10 tyrosine can be in either the A or B positions in the deoxy species (panel a). The B10 tyrosine forms H-bonds with the heme-bound dioxygen molecule only when it is in the A position. On the contrary, it forms a H-bond with the heme-bound CO only when it is in the B position. Binding an oxygen molecule to the first subunit introduces an allosteric structural transition that causes both the B10 tyrosine residues to be locked in the A position (panel b). If the second subunit binds another oxygen molecule, the B10 tyrosine, which is in position A, forms two H-bonds with the oxygen molecule (panel c). On the contrary, if the second subunit binds a CO molecule, the H-bond between the B10 tyrosine and the heme-bound CO cannot be established because the B10 tyrosine is locked in position A (panel d). The distinct quaternary structure of each subunit in the various ligation states of the HbN dimer is schematically illustrated by a square-shaped or a circular-shaped subunit.

Owing to the intrinsic difference in the hydrogen bonding capability and the binding geometry of CO (linear) and O_2 (bent), the stabilizing interactions between the bound CO and the B10 tyrosine in the second subunit are too weak to lock the second subunit in the closed conformation. Consequently, it is energetically more favorable for the CO-bound subunit to adopt an open conformation such that the interfacial stabilization energy between the two subunits can be maintained (Figure 6d).

A Two-State Model. The two-state model is analogous to that proposed for human hemoglobin by Monod, Wyman, and Changeux, although the molecular rearrangements underlying the conformational transition may be of a very different nature.[14] In this model, the B10 tyrosine can be in either the A position or the B position (Figure 7). When the B10 tyrosine is in the A position, it favors the hydrogen-bonding interaction with the heme-bound O_2, which has a bent structure, but not with the heme-bound CO, which has a linear geometry. On the other hand, when it is in the B position, it favors a hydrogen bond to the linear CO but not to the bent O_2. Consequently, the Fe−O_2 stretching frequency at 560 cm^{-1} and the Fe−CO stretching frequency at 500 cm^{-1} are assigned to the conformations in which the B10 tyrosine is in the A position. On the other hand, the Fe−CO stretching frequency at 535 cm^{-1} is assigned to a conformation in which the B10 tyrosine is in the B position. The B10 tyrosine in the ligand-free form fluctuates between the A and B positions (Figure 7a). If the first subunit of the dimer binds an O_2 molecule, it locks the B10 tyrosine in the A position through the strong H-bonding interaction. The enclosure of the heme pocket around the heme-bound O_2 introduces topological changes to both subunits (Figure 7a,b) through an allosteric structural transition. The structural change in the second subunit forces the B10 tyrosine to be in the A position (Figure 7b). If the second subunit of the dimer binds another O_2 molecule, a single Fe−O_2 stretching mode is present at 560 cm^{-1} because both subunits are in the A conformation (Figure 7c). If the second subunit binds a CO molecule, it forms the mixed-ligand dimer with only one Fe−CO stretching mode at 500 cm^{-1} that is associated with the A conformation (Figure 7d).

Since the mixed-ligand species resembles the intermediate ligation state during the oxygenation of the dimeric HbN, the data provide the first experimental evidence for an intermediate ligation state that is critical for a ligand-linked allosteric structural transition. There are several protocols one could use to differentiate the three-state mechanism from the two-state mechanism. A straightforward approach is first to trap the fully oxygenated protein in a solid matrix (e.g., a sol−gel)[48−50] and then to purge off the heme-bound O_2 with an inert gas (e.g., N_2) while the conformation of the protein is held in the oxy state (Figure 6c or 7c). If the protein is subsequently subjected to CO, a single band at 535 cm^{-1} is expected for the two-state model (Figure 6) whereas a single band at 500 cm^{-1} is expected for the three-state model (Figure 7).

Three decades ago, Perutz proposed that the allosteric structural transition in human hemoglobin is initiated by a structural movement along the iron−histidine bond on the proximal side of the heme in response to ligand coordination.[14] This model has served as the foundation for our understanding about the allosteric mechanism of hemoglobins since then, although several new allosteric transition mechanisms have been proposed for other hemoglobins in recent years. The data presented here for HbN reveal a novel intersubunit communication mechanism that is triggered by the H-bonding interaction between the B10 tyrosine and heme-bound ligand. The ligand-induced conformational change provides a mechanism by which this fascinating family of proteins regulates its ligand-binding properties, as well as its physiological functions.

Acknowledgment. I thank Dr. Denis L. Rousseau for many helpful discussions and Dr. Michel Guertin for providing the protein sample. This work was supported by the National Institute of Health Research Grant HL65465.

Supporting Information Available: The raw Raman spectra of HbN obtained in the ligand replacement experiments. This material is available free of charge via the Internet at http://pubs.acs.org.

References and Notes

(1) Weber, R. E.; Vinogradov, S. N. *Physiol. Rev.* **2001**, *81*, 569.
(2) Bolognesi, M.; Bordo, D.; Rizzi, M.; Tarricone, C.; Ascenzi, P. *Prog. Biophys. Mol. Biol.* **1997**, *68*, 29.
(3) Riggs, A. F. *J. Exp. Biol.* **1998**, *201*, 1073.
(4) Appleby, C. A. *Annu. Rev. Plant Physiol.* **1984**, *35*, 443.
(5) Andersson, C. R.; Jensen, E. O.; DJ, L. L.; Dennis, E. S.; Peacock, W. J. *Proc. Natl. Acad. Sci. U.S.A.* **1996**, *93*, 5682.
(6) Watts, R. A.; Hunt, P. W.; Hvitved, A. N.; Hargrove, M. S.; Peacock, W. J.; Dennis, E. S. *Proc. Natl. Acad. Sci. U.S.A.* **2001**, *98*, 10119.
(7) Wittenberg, J. B.; Bolognesi, M.; Wittenberg, B. A.; Guertin, M. *J. Biol. Chem.* **2002**, *277*, 871.
(8) Pesce, A.; Bolognesi, M.; Bocedi, A.; Ascenzi, P.; Dewilde, S.; Moens, L.; Hankeln, T.; Burmester, T. *EMBO Rep.* **2002**, *3*, 1146.
(9) Hardison, R. *J. Exp. Biol.* **1998**, *201*, 1099.
(10) Bellelli, A.; Brunori, M. *Methods Enzymol.* **1994**, *232*, 56.
(11) Rodgers, K. R.; Spiro, T. G. *Science* **1994**, *265*, 1697.
(12) Jayaraman, V.; Rodgers, K. R.; Mukerji, I.; Spiro, T. G. *Science* **1995**, *269*, 1843.
(13) Ackers, G. K.; Doyle, M. L.; Myers, D.; Daugherty, M. A. *Science* **1992**, *255*, 54.

(14) Perutz, M. F.; Wilkinson, A. J.; Paoli, M.; Dodson, G. G. *Annu. Rev. Biophys. Biomol. Struct.* **1998**, *27*, 1.
(15) Royer, W. E., Jr.; Hendrickson, W. A.; Chiancone, E. *Science* **1990**, *249*, 518.
(16) Yonetani, T.; Park, S. I.; Tsuneshige, A.; Imai, K.; Kanaori, K. *J. Biol. Chem.* **2002**, *277*, 34508.
(17) Henry, E. R.; Bettati, S.; Hofrichter, J.; Eaton, W. A. *Biophys. Chem.* **2002**, *98*, 149.
(18) Imai, K.; Tsuneshige, A.; Yonetani, T. *Biophys. Chem.* **2002**, *98*, 79.
(19) Minning, D. M.; Gow, A. J.; Bonaventura, J.; Braun, R.; Dewhirst, M.; Goldberg, D. E.; Stamler, J. S. *Nature* **1999**, *401*, 497.
(20) Goldberg, D. E. *Chem. Rev.* **1999**, *99*, 3371.
(21) Appleby, C. A. *Sci .Prog.* **1992**, *76*, 365.
(22) Wittenberg, J. B. *J. Biol. Chem.* **1974**, *249*, 4057.
(23) Poole, R. K.; Hughes, M. N. *Mol. Microbiol.* **2000**, *36*, 775.
(24) Cramm, R.; Siddiqui, R. A.; Friedrich, B. *J. Biol. Chem.* **1994**, *269*, 7349.
(25) Crawford, M. J.; Goldberg, D. E. *J. Biol. Chem.* **1998**, *273*, 12543.
(26) Gardner, P. R.; Gardner, A. M.; Martin, L. A.; Salzman, A. L. *Proc. Natl. Acad. Sci. U.S.A.* **1998**, *95*, 10378.
(27) Gardner, P. R.; Gardner, A. M.; Martin, L. A.; Dou, Y.; Li, T.; Olson, J. S.; Zhu, H.; Riggs, A. F. *J. Biol. Chem.* **2000**, *275*, 31581.
(28) LaCount, M. W.; Zhang, E.; Chen, Y. P.; Han, K.; Whitton, M. M.; Lincoln, D. E.; Woodin, S. A.; Lebioda, L. *J. Biol. Chem.* **2000**, *275*, 18712.
(29) Franzen, S.; Roach, M. P.; Chen, Y.-P.; Dyer, R. B.; H., W.; Woodruff, W. H.; Dawson, J. H. *J. Am. Chem. Soc.* **1998**, *120*, 4658.
(30) Antonini, E.; Brunori, M. Chemistry of Myoglobin and Hemoglobin. *Hemoglobin and myoglobin in their reactions with ligands*; Elsevier North-Holland: Amsterdam, 1971; Vol. 21; p 70.
(31) Hirota, S.; T., L.; Phillips, G. N.; Olson, J. S.; Mukai, M.; Kitagawa, T. *J. Am. Chem. Soc.* **1996**, *118*, 7845
(32) Tomita, A.; Hirota, S.; Ogura, T.; Olson, J. S.; Kitagawa, T. *J. Phys. Chem. B.* **1999**, *103*, 7044.
(33) Nagai, K.; Kitagawa, T. *Proc. Natl. Acad. Sci. U.S.A.* **1980**, *77*, 2033.
(34) Friedman, J. M.; Rousseau, D. L.; Ondrias, M. R.; Stepnoski, R. A. *Science* **1982**, *218*, 1244.
(35) Coletta, M.; Boffi, A.; Ascenzi, P.; Brunori, M.; Chiancone, E. *J. Biol. Chem.* **1990**, *265*, 4828.
(36) Royer, W. E., Jr. *J. Mol. Biol.* **1994**, *235*, 657.
(37) Heaslet, H. A.; Royer, W. E., Jr. *Struct. Fold Des.* **1999**, *7*, 517.
(38) Moens, L.; Vanfleteren, J.; Van de Peer, Y.; Peeters, K.; Kapp, O.; Czeluzniak, J.; Goodman, M.; Blaxter, M.; Vinogradov, S. *Mol. Biol. Evol.* **1996**, *13*, 324.
(39) Milani, M.; Pesce, A.; Ouellet, Y.; Ascenzi, P.; Guertin, M.; Bolognesi, M. *EMBO J.* **2001**, *20*, 3902.
(40) Milani, M.; Savard, P. Y.; Ouellet, H.; Ascenzi, P.; Guertin, M.; Bolognesi, M. *Proc. Natl. Acad. Sci. U.S.A.* **2003**, *100*, 5766.
(41) Pesce, A.; Couture, M.; Dewilde, S.; Guertin, M.; Yamauchi, K.; Ascenzi, P.; Moens, L.; Bolognesi, M. *EMBO J.* **2000**, *19*, 2424.
(42) Yeh, S. R.; Couture, M.; Ouellet, Y.; Guertin, M.; Rousseau, D. L. *J. Biol. Chem.* **2000**, *275*, 1679.
(43) Couture, M.; Yeh, S. R.; Wittenberg, B. A.; Wittenberg, J. B.; Ouellet, Y.; Rousseau, D. L.; Guertin, M. *Proc. Natl. Acad. Sci. U.S.A.* **1999**, *96*, 11223.
(44) Ouellet, H.; Ouellet, Y.; Richard, C.; Labarre, M.; Wittenberg, B.; Wittenberg, J.; Guertin, M. *Proc. Natl. Acad. Sci. U.S.A.* **2002**, *99*, 5902.
(45) Pathania, R.; Navani, N. K.; Gardner, A. M.; Gardner, P. R.; Dikshit, K. L. *Mol. Microbiol.* **2002**, *45*, 1303.
(46) Mukai, M.; Mills, C. E.; Poole, R. K.; Yeh, S. R. *J. Biol. Chem.* **2001**, *276*, 7272.
(47) Das, T. K.; Friedman, J. M.; Kloek, A. P.; Goldberg, D. E.; Rousseau, D. L. *Biochemistry* **2000**, *39*, 837.
(48) Bruno, S.; Bonaccio, M.; Bettati, S.; Rivetti, C.; Viappiani, C.; Abbruzzetti, S.; Mozzarelli, A. *Protein Sci.* **2001**, *10*, 2401.
(49) Khan, I.; Shannon, C. F.; Dantsker, D.; Friedman, A. J.; Perez-Gonzalez-de-Apodaca, J.; Friedman, J. M. *Biochemistry* **2000**, *39*, 16099.
(50) Shibayama, N.; Saigo, S. *J. Mol. Biol.* **1995**, *251*, 203.
(51) Couture, M.; Das, T. K.; Lee, H. C.; Peisach, J.; Rousseau, D. L.; Wittenberg, B. A.; Wittenberg, J. B.; Guertin, M. *J. Biol. Chem.* **1999**, *274*, 6898.
(52) Das, T. K.; Couture, M.; Ouellet, Y.; Guertin, M.; Rousseau, D. L. *Proc. Natl. Acad. Sci. U.S.A.* **2001**, *98*, 479.
(53) Das, T. K.; Lee, H. C.; Duff, S. M.; Hill, R. D.; Peisach, J.; Rousseau, D. L.; Wittenberg, B. A.; Wittenberg, J. B. *J. Biol. Chem.* **1999**, *274*, 4207.
(54) Das, T. K.; Weber, R. E.; Dewilde, S.; Wittenberg, J. B.; Wittenberg, B. A.; Yamauchi, K.; Van Hauwaert, M. L.; Moens, L.; Rousseau, D. L. *Biochemistry* **2000**, *39*, 14330.
(55) Couture, M.; Das, T. K.; Savard, P. Y.; Ouellet, Y.; Wittenberg, J. B.; Wittenberg, B. A.; Rousseau, D. L.; Guertin, M. *Eur. J. Biochem.* **2000**, *267*, 4770.
(56) Ramsden, J.; Spiro, T. G. *Biochemistry* **1989**, *28*, 3125.